The Yellowstone Fires as Observed by SIR-C SAR

Eric Rignot, 1 Don Despain*, and Francesco Holecz

Jet Propulsion laboratory, California Institute of Technology, 4800 oak Grove Drive, Pasadena CA 91109-8099

* National Biological Service, Midcontinent Ecological Research Center, Greater Yellowstone Field Station, Box 168 Yellowstone National Park, Wyoming 82190

Abstract. In 1988, nearly one million hectares of forest burned in the Greater Yellowstone area. Six years later, the fire scars are still visible in the radar images acquired at C- (5.6 cm) and L- band (24 cm) frequencies, with both like and cross-polarized returns by the Spaceborne Imaging Radar C (SIR-C). The radar imagery was registered to a digital elevation model of the area, rectified for geometric distortions, corrected for calibration errors introduced during processing by assuming a flat Earth model, and corrected for natural variations in radar backscatter of the forest with the local incidence angle of the radar illumination. The radar data were then employed to produce a land cover classification) using a supervised Bayesian classifier. Good results were obtained even in areas of pronounced topographic relief. Comparisons with a map of the 1988 fires obtained from Landsat imagery, atria] photos, and ground surveys reveal SIR-C single date imagery identifies burned forests with more than 78% accuracy. Various levels of fire severity corresponding to different levels of crown biomass arc differentiated within the burn. In live forests, SIR-C separates forests which differ in density, structure, and crown biomass. L-band Cxoss-polarized data arc most effective to map the fire scars due to their sensitivity to crown biomass. C- band cross-polarized data show less contrast between burn and non-burn. P-band data collected by an airborne system show no fire scars at like polarization because they interact with tree-trunks and the larger branches, which, despite being killed by the fires, were not consumed by them and arc still acting as efficient scatterers after the fire. These SIR-C results demonstrate the utility of long wavelengths, multiple polarization, imaging radars to study large wildland fires. Operating independent of solar illumination, cloud cover, and fire smokes, these instruments could detect fore.st burn even as the fires progress, map fire severity, provide synoptic views of the forest remaining burning fuels, and help study post-burn forest regeneration.

introduction

In 1988, the Yellowstone National Park (YNP) was affected by one of the largest complex of fires in the Northern Rockies in the last 50 years (Christensen et al, 1989). The fires attracted intensive media attention and deep public concern. Because they were so extensive, and provided a unique opportunity to study forest regeneration, the 1988 fires also generated immense scientific interest. Although they were vast, these fires were not at all unprecedented (Romme and Despain, 1989a and b). The unusual extent of the 1988 fires was the consequence of extreme drought and persistent high winds on the Yellowstone Plateau in the summer of 1988, combined with the presence of an extensive cover of highly flammable old-growth forests that had developed undisturbed since the early 1800's (Romme and Despain, 1989).

Several post-fire studies estimated how much of the Greater Yellowstone area was burned by the fire, the intensity of the fire, the distribution of the burns, and so on (Despain et al., 1989; Rothermel et al. 1994). The results revealed a complex mosaic of forest stands with various degrees of burn, with spatial scales ranging from a few meters to several kilometers. In some areas, the fire consumed all the needles and some small twigs of the tree and sapling crowns. This all occurs in about 10-40 seconds (Despain et al. 1996). During this time the litter, duff and rotten logs on the forest floor would be ignited and the outside 2-3 cm of both standing and fallen the dead trees would be charred, creating a canopy burn. The dry duff and rotten logs and the dry dead branches up to 10 cm diameter would be consumed over the next hour or two. In other areas, the fire consumed the crowns of some trees, merely scorched the crowns of others, girdled others that would die over the next three years, and crept around on the ground surface causing very little damage to the trees and

burning patches of duff and rotten logs, creating a mixed burn (Despain et al., 1989). A central area of canopy burn would typically be surrounded by mixed burn. Outside the central area, canopy burn or surface burn would occur in isolated spots (Despain et al., 1989). Patches of unburned forest could also be left within a large area of burn due to the erratic fire behavior or the joining of several separate fires.

Two of the most important questions asked during the fire were: how much land has burned and where was the perimeter of the different fires at the end of each burning period? Answering those questions was difficult because ground surveying was risky and optical imagery could not be used through the smoke, especially in those areas where smoke from one fire obscured another fire. Infra-red S[>11S01'S were utilized at night over the most critical areas but only when they were not needed on fires with higher priority. The in fra-red images are difficult to interpret and rectify to maps because they rely on temperature differences. They mostly record not spots along the most recently burned fire fronts. Estimates of burned area could vary widely depending on the definition of burned area and the uncertainty in the means of measuring it. The biggest problem ultimately became the shear magnitude of the fires. Aircraft simply could not cover the entire area burned in a suitable time frame. The location of the fire perimeter is very important to those involved in the constant planning needed during the suppression efforts. The planning teams need to know how many resources will be needed for the next shift and where they will be needed. They .31s0 need that information to provide for the safety of the fire fighters and any people in the path of the fire.

After the fire is out, land managers need to know how much of their stewardship has been burned at the various intensities in order to provide for any needed rehabilita-

tion or to plan for the changes made in the natural resources available to the different consumers, both human and nonhuman. Researchers interested in questions regarding fire effects on vegetation, animal populations and behavior and hydrology need accurate information on the location and intensity of the fires. This information is also of interest to those studying landscape ecology. Knowledge of where the [ire was at various times is useful to those studying fire behavior as it is affected by weather and fuel conditions.

No spaceborne Synthetic Aperture Radar (SAR) was operating in 1988 to survey the Yellowstone fires. A SAR instrument would have helped survey the fires because it operates independent of solar illumination, cloud cover, and fire Slink, and senses variations in canopy structure and biomass. In October 1994, the Shuttle Imaging Radar C, a spaceborne radar operating at C- and L-band frequency, with bet]] vertical and horizontal polarizations, provided the first multi-channel spaceborne images of Yellowstone, six years after the last major fire disturbances. The main objectives of this study were to determine whether SIR-C SAR could still see the fire scars, how accurately it could map them, whether different levels of fire severity could be differentiated, how the results would compare to those obtained by earlier studies, what additional information SIR-C SAR could procure about burned and unburned areas, and what radar channels among those studied were essential and most efficient to map forests damaged by wild fires.

Study Site

Yellowstone National Park (YNP) is the oldest national park in the world. It lies mostly in the northwestern corner of Wyoming and includes about 890,000 ha, parts of southwest Montana and southeast Idaho. It consists of large volcanic plateaus

of rhyolitic rocks surrounded by mountains of predominantly andesitic rock. 'T11(: weathered products of these rock types produce contrasting soils, Andesite produces soils with good fertility and good water holding capacity while rhyolite produces soils that arc infertile and dry. Winters are cold, lasting from mid November to mid March. Summers are often dry, usually lasting from July through August. Most of the park is coved with seral forests dominated by lodgepole pine (Pinus contorta) and Engelmann spruce (Pica engelmannii) and sill.ml])i]le fir (Abies lasiocarpa) arc climax species. Other stands include whitebark pine (Pinus albicaul is) and douglas-fir (Pseudotsuga menziesii). Lodgepole pine is most common on the rhyolite soils. It can form climax stands on the driest sites. Andesite soils are mostly covered with douglas-fir at lo wer elevations, lodgepole pine or spruce and fir forest at mid and upper elevations and whitebark pine above 2620 m. Most of the forest is in some stage of succession following natural disturbance, especially fire (Despain, 1990).

The continuous process of fire succession breaks into five recognizable stages based on stand structure (Despain, 1977 and 1990). In the initial stage, fire ignites from lightning in old-growth forest, of lodgepole pine, Engelmann spruce and subalpine fir and burns the forest, overstory. Seeds protected from the fire in fire-rcsistallt lodgepole pine cones are released after the fire and initiates early succession (Despain et al., 1996). For the first 5 years, the new seedlings are scarcely noticeable on the forest floor but then they begin to grow about 30 cm per year depending on site conditions. In stands that had an adequate crown seed bank, the seedlings can be quite dense. In others they arc often sparse at first (Anderson and Romme, 1991). This stage usually lasts 20-40 years and is called LP0 until canopy closure occurs. In the next stage, 1,1'1, 50-100 years post-burn, the pines form dense, homogeneous stands, with trees 30-50 feet high. In the 3rd stage, LI '2, 150-300 years post-burn,

the IO(lg('pole pines thin out, and the precursors of t he second generation forest o f Engelmann spruce and subalpine fir arc noticeable on fertile soils. The original trees eventually begin to die in stage LP3, 3(1(1 years post-burn, leaving a mixed canopy ()(lodgepole pine, Engelmann spruce and subalpine fir, with large gaps in the canopy, a widely diverse understory, and large amounts of dead and flammable materials on the forest floor which render the forest again vulnerable to fire. Time to progress from one stage to another and the characteristics of the forest in each stage is dependent on site conditions. On good soils with adequate moisture the process goes faster and is able to Support, a higher stand biomass. Engelmann spruce and subalpine fir can st art with the lodgepole pine in moist places and higher elevations if there is a nearby Seed Soul'cc, Given enough time, the climax stage of Engelmann spruce and subalpine fir forest is eventually reached. On extremely dry infertile soils, however, lodgepole pines dominate the underst ory, resulting instead in a multiaged lodgepole pine canopy with only a moderate dead and downed fuel component and no spruce - fir understory (stage LP). Very few stands of climax stage spruce and fir exist at, YNP because the forest typic ally b urns before it reaches that stage.

Fire occurrence and activity are much greater in old-growth forests (1,1'3) than in initial(LP0), successional (LP1-LP2), and multiaged (LP) lodgepole pine forests (Renkin and Despain, 1992). Old-growth forests include more dead and down woody fuel loading than the other stands, and more live fuel loading with an understory of Engelmann spruce and subalpine fir regeneration. Early stages of forest regeneration yield stands homogeneous in tree height and density because trees arc even-aged. Stands of similar age however frequently differ in density because of site conditions.

Methods

SIR-C imaged YNP 011 October 7, 19\J4 during its second mission (SRL-2) on orbit 39 of the space shuttle Endeavor. The false color composite image shown in Figure 1 is centered at 44.59°N, 11 10.63°W. Image size is 97.1 km by 89.6 km. The incidence angle of the radar illumination is 58.7° at the image center. Yellowstone Lake is visible as a large dark area at the bot tom of the scene. North is on top. SIR-C is flying from top to bottom, looking to its right, and illuminating a 45-km wide swath.

The SIR-C data were georeferenced, geometrically rectified, and re-calibrated using a digital elevation model (DEM) from the U.S. Geological Survey at 7.5 minute spacing (pixel size about 30 m), in Universal Transverse Mercator (UTM) projection. Re-calibration of the data was necessary because the SAR data were initially processed assuming a flat earth model, which introduces biases in the modeled receiver power at the antenna (Holecz et al., 1994). As a result of the radiometric corrections, topography induced variations in radar backscatter were significantly reduced, as shown in Figure 2, and geometric distortions of the SAR imagery in areas of rugged terrain were eliminated. The radar brightness of the forest was however still noticeably influenced by topography in areas of steep surface slope because radar backscatter also naturally varies with the local incidence of the radar illumination. The limited precision of the DEMs used for geocoding of the SAR imagery showed up in the results. Discontinuities in surface slope resulting from the digitization process of the DEMs introduced a faint miring in parts of the geocoded SAR imagery. In areas of complex topography, the 30 m spatial resolution of the DEM was not sufficient to yield accurate radiometric corrections. In addition to the difficulties inherent to the DEMs, the radiometric calibration of the data was affected by a ± 1dB uncertainty in antenna gain across-track caused by a ±0.1° uncertainty in the roll angle of the Sill-(; antenna along-track (Freeman et al., 1995). C-band HV-polarization data (horizontal

transmit and vertical receive) are not utilized in this study because these data were affected by high system noise in the far swath of the scene caused by data acquisition at, a very large incidence.

Georeferencing of the radar imagery was evaluated 011 22 grou nd control points, and indicated a precision of better than one pixel spacing. The geocoded data overlaid perfectly with the data stored on a Geographical Information System (GIS) built around the GRASS software and utilized at the Division of Research, YNP.

To further reduce the influence of surface topography on the SAR signal, we normalized the radar data by the cosine of the local incidence angle of the radar illumination calculated from the DEM and the SAR imaging geom etry. This type of correction is justified for radar scattering fro m vegetation when volume scat tering interactions dominate the radar returns (e.g. Bernard and Vidal-Madjar, 1989), which is the case at C- and L- band frequencies for the forests imaged in this scene as discussed later on in this paper. The results show a significant reduction of surface topography -induced variations in radar backscatter, whit.11 in turn validates our cosine-law compensation (Figure 3). The effect of topography is only visible in areas of excessive slope (canyon, mountain ridges) where the surface is actually shadowed from the radar illumination.

To classify the SIR-C data, training areas were selected in the SA R scene based on the color contrast between various types of land cover in the false-color composite Sill-C images. Labeling of each training area into a type of land cover was based on prior classifications of the scene (Figure 6) and on the interpretation of the radar scattering characteristics of each training area. A total of 12 training sites wercsclcc.ted, later regrouped into 8 categories of land cover. These categories are: 1) open water, 2) open meadow/non-forest; 3) canopy bill'11; 4) mixed burn; 5) sp arse/dry forest; 6)

sparse forest,; 7) intermediate forest; and 8) dense forest,. Areas of excessive surface slopes were masked out, appearing white in Figure 5, because they correspond to areas shadowed from the radar illumination. The multi-channel statistics of the 12 training sites were then utilized to classify the entire scene using a Maximum-A-Posteriori Bayesian classifier (Rignot and Chellappa, 1992). The results, color coded in 8 categories, are shown in Figure 5. The backscatter characteristics and land cover categories of each training site are summarized in Table 1.

In September 1989, the NASA/JPL AIRSAR instrument imaged YNP, in an area cutting along the middle of the SIR-C swath, in the cast-west, direction, just one year after the fire. The radar data were collected simultaneously at three frequencies (C, 1,-, and P-band (68 cm)), with the full polarimetry, across a 10 **Ii Ill** swath, at about 10 m pixel spacing. In this type of imagery, the radar illumination angle varies from 20° in the Ijcar-range to > 55° in the far-range, whereas in the SIR-C imagery the illumination angle remained at about 58° across the entire scene. The entire AIRSAR data take was 50 km long, but we here only discussed a 10 km portion of the imagery acquired near the Old Faithful Lodge, in the center-left portion of the SIR-C scene. The radar data were projected onto ground-range, assuming a flat Earth model, and were analyzed to determine the mode of scattering of the radar signals at the three different radar frequencies. This analysis utilizes a mathematical decomposition of the polarimetric signal into its eigml-vectors and eigen-values, known as Cloude decomposition (van Zyl,] 992). The three canonical form of radar scattering are single bouncing, double bouncing, and multiple scattering (or volume scattering). The contribution of each canonical form of scattering to total backscatter is shown, respectively, in blue, red and green in Figure 4. The decomposition does not identify a type of land cover but indicates how the radar signals interact with the surface,

which in turn helps in the scientific analysis of the radar data.

Landsat TM provided its first cloud-free image of the 1988 YNP fires on October 2, 1988. When those data became available to the EROS Data Center, the image was georectified and a normalized difference vegetation index was calculated for each pixel. The resultant layer was subjected to an unsupervised classification. Classes that were obviously burned areas were then used as a mask and a second unsupervised classification was run. Post,-fire air-photos were then used to visually combine the 32 resultant classes into 7 classes according 10 3 tree density classes (dense, moderate and sparse) and two bum intensity classes (canopy and mixed), plus burned nonforest (Ohlin and Despain, manuscript in preparation, 1996). The resulting map of fire severity is shown in Figure 6. This map also shows 4 successional stages of live forest (LP1, LP2, LP3 and LP), stands domina ed by dougl as-fir, stands dominated by white bark, and opcu water, The class LP(includes burned areas colored either red (canopy burn) or orange (mixed burn).

Aerial photogra phs were also available over the entire park to help interpret the radar observations. Each image is about 5 km by 5 km, and individual trees may be resolved by inspection of the data under the microscope. These photos were used to locate the limits of the burn, and study spatial variations in forest density and tree species.

Results

Scattering mechanisms

We first discuss the radar scatter ng mechanisms recorded in the 1989 AIR SAR imagery shown in Figure **4.** Significant changes in sc attering mechanisms occur between C-, L- and P-band frequencies. At C-band, burned areas are well separated from live

forests. Live forests appear green, which means volume scattering interactions dominate, whereas burned areas appear blue, which means single bouncing dominates. In live forest, the recorded polarimetric signal is consistent with volume scattering interactions from the needles, twigs and branches of the upper forest canopy. In burned forests, single scattering events must be caused by direct reflections of the radar signals on the ground layers.

At L-band, live forest appears greener, which means volume scattering interactions are enhanced compared to C-band. The more bluish tone of the forest at C-band suggest a higher portion of the backscattered energy resulted from direct reflections of the radar signals from the top of the canopy. Burned areas are still dominantly blue at L-band, but a green component is now present. Forest regrowth was negligible in 1989 and is unlikely to explain that green component. Volume scattering must originate from scattering by the many dead branches still present on standing dead trees killed by the fires. Numerous parts of the forest also show double bounce reflections. Scattering models indicated double bouncing is mostly associated with reflections on the corner reflectors formed by the tree-trunks and the ground. The magnitude of these interactions increases when the ground is wetter or smoother, the trunks are tall, wide and wet, attenuation of the radar signals through the forest canopy is reduced, and terrain slope facilitates reflections toward the radar looking direction (van Zyl, 1 993). In live forest, enhanced double bouncing probably occurs in areas of lower forest density. Most lodgepole pine forests of YNP have low density because the rhyolite soils are nutrient poor and dry.

At P-band, volume scattering and double bouncing dominate the radar returns from live forest. Larger patches of forest are colored red, suggesting enhanced interactions

with the tree-trunks . B urned forests are still blue but the green and red com ponents arc larger than at L-band. Fire scars arc in fact no longer visible at, P-band HH- and VV-polarization, and only the P-band HV data (here coil'csl)ollclillg" to the green component) separates burn fro n un burn. At P-band, the radar signals dominantly interact with the larger tree branches and the trunk-ground reflectors (Beaudoi n et al., 1 994). our results suggest this is even true after trees and large branches are killed by a fire even though their dielectric constant must be lower than in live vegetation.

We could not run the same type of decomposition with the SIR-C data because those data comprised only two channels (HH and **H V),** The complete polarimetry is needed to analyze radar scattering mechanisms. It is however likely the results obtained with AIRSAR still apply for Silt-C because both images were acquired in similar conditions and forest regrowth was limited between 1989 and 1994.

SIR-C Classification of Land Cover Types

1 Burned areas arc clearly visible in the false-color composite images obtained from Sill-C (Figure 1-3). They appear dark red, meaning low radar returns at L-band 1111 and HV and high radar returns at C- band HH. These areas are not well separated from live forests at C-band HH, but a difference in backscatter exist at C-band HV, consistent with the AIRSAR results. Canopy burn and mixed burn (Figure 6) yield different levels of radar backscatter (Table 1). Mixed burn has higher L-band 1111 and HV backscatter, consistent with a greater amount of crown biomass. Canopy burn has very low HV backscatter.

Areas appearing yellow in Figure 1-3 correspond to canopy burn in sparse forests. These stands are radar-bright, at L-band HH and especially at C-band HH where

they represent the brightest type of forest in the entire scene. such a patch of forest is present in the north-west sector of the SAR scene, west of' West-Yellowstone, in an area of infertile soils of sand and gravel with little forest floor vegetation. half of that forest burned in 1988 and shows up as bright yellow in the SIR-C false-color composite image. The other half appears bright green-blue. Strong radar returns are recorded at **11** H-polarization in the burned areas, suggesting strong double boun ce scattering. Stands of similar characteristics in the Sill-C image are present within the area covered by the AIR SAR scene and show pronounced double bounce scattering at P-band, but also at L- and C-band in the Cloude decomposition. These forests are distinct from live forests because both the combined absence of a thick forest canopy and of fewest floor vegetation greatly enhances double bounce reflections from trun - ground reflectors. This type of vegetation was labeled as canopy burn in Figure 5.

The fire! map illf'erred from the SIR-C data (Figure 5) compares well with the map in ferred from Landsat TM data and ground surveys (Figure 6). On a pixel per pixel basis, more than 78%, of the burned forests in Figure 6 are correctly classified as burn in Figure 5. The agreement between different levels of fire severity is comparatively less as Sill-C tends to overestimate the fraction of mixed burn compared to canopy 1)111' 11. Canopy burn in the SIR-C classificat ion correspond to areas of lowest crown biomass, meaning where fire destruction was the greatest. In the Landsat classification, canopy burn corresponds to areas where patches of live vegetation could still be found in 1988. Canopy burn in the Landsat definition therefore includes a larger fraction of burned forests. Both classifications complement rather than contradict each other.

In the highest mountain ranges o the south-east, sollll-west and north-east of the

park, SIR-C misclassified patches of live forest as burned forests. These forests comprise a mixture of douglas fir trees and TIoII-forest, and are therefore of" very low crown biomass. Confusion with burned forests is unavoidable based on radar backscatter alone, yet wild fires are highly unlikely in these high-elevation regions. Similarly, image pixels at the transition between forest and meadows or open waler were mis-classified as burn in Figure 5. This type of error is caused by edge effects from the surrounding forest and is also be easily recognized in the classification map.

Several patches of burned forests were]Ilis-labeled as live forest by S1 R-CSAR. 011 example is the large patch of mixed burn in the north-east section of the scene, north of a large meadow. Perhaps forest regrowth has been more significant in this region. Forest regrowth varies widely across the park depending on soil conditions and post, -burn bank seeds. Seedlings may vary from a few tens of centimeters in height on nutrient-poor dry soils to 1-2 m on nutrient-rich wet soils. Further studies are needed to determine whether this provides a reasonable explanation for the difference between SIR-C and Landsat classifications. Another possibility, however, is the radar data were not calibrated well enough in this far-range portion of the scene. Fire scars are actually clearly visible in the false-color composite images (Figure 1-3), but the forest appears brighter than on average and the classification assigns a higher-than-expected percentage of live forests in this area.

Another source of confusion between live and burned forest is the forest we labeled very sparse lodgepole pine forest (Figure 5). The radar backscatter characteristics of this forest suggest a very low crown biomass (Table 1), because the radar response at 1,-band HV is similar to that of mixed burn. Most of this forest occurs above 2600 m elevation, in a region where soil conditions were notably drier than in the rest of the

park in October 1994 and where air temperatures are on average colder during the year. Forest development could therefore be more limited, and vegetation canopies may be drier. Inspection of aerial photos revealed the presence of numerous douglas fir trees in this area, so tile difference n radar backscatter could also be due to a difference in forest structure.

The classification of the SIR-C data in live forest produced classes that are weakly correlated with forest age along the fire succession (Figure (i). The SAR classes reflect differences in crown biomass, canopy structure, and perhaps water content of the vegetation. Fire succession produces even-aged stands, but forest density is known to vary widely between similar stands depending on the initial seedling densi ties and soil conditions. It is therefore not surprising the SAR classes do not match directly into successional stages.

Detailed forest inventories will be conducted in the future to estimate crown biomass and to utilize the Sill.-C data to obtain quantitative estimates of crown biomass. Similar studies conducted in other types of pine forests have demonstrated L-band HV was highly correlated with crown biomass in mono-specie forests (Beaudoin et al., 1994). Combined with the SIR-C data, these forest inventories will help estimate the live burning fuels of the forest, which is of interest to fire spread models such as EMBRY (Hargrove et al., manuscript in preparation) and FAR SITE. This type of information would be a great use to fire behavior analysts working on fire fighting overhead teams and those responsible for projecting natural fires in the western wilderness areas.

Conclusion

In 1988, fire maps could only be assembled several months after the fire season because no clol]d-free satellite images were available during the fire season. Numerous ground surveys were also necessary to validate the interpretation of the satellite imagery. For many months, it was not clear how much of YNP was burned by tilt' fire, what were the patterns of burn severity exhibited by the fires, and how the fires progressed.

A satellite SAR would greatly improve the results and help monitor fire progression because it operates independent Of fire smokes, solar illumination, and cloud cover. This study demonstrates SAR can map burned forests and fire severity very well due to its sensitivity to crown biomass, even if limited to single date imagery. Mult,i-elate imagery would certainly facilitate the labeling of classes of radar backscatter into different categories of burn, and improve the overall classification accuracy, For optimum mapping, cross-polarized signals acquired at a long radar wavelength appeared preferable. No spaceborne SAR currently offers that possibility.

Acknowledgements

This work was partly carried out at the Jet Propulsion Laboratory, California Institute of Technology, under a contract with the National Aeronautics and Space Administration. The authors would like to thank all the people at the Jet Propulsion Laboratory involved with the processing and generation of the SIR-C SAR products.

References

Beaudoin A. and 9 others (1 994) Retrieval of forest biomass from SAR data, *Int. J. of Rem. Sens.* 15(4), 2777-2796. Bernard, R. and D. Vidal-Madjar (19S9) C-band radar cross section of the Guyana rain forest: possible use as a reference target for spaceborne radars, *Rem. Sens. Environ.* 27, 25-36.

Christensen, N.L., J.K. Agee and 11 others (1 989) Interpreting the Yellowstone fires of 1988, *Bioscience*, 39, 678-685.

Despain, D., **A.** Rodman, 1'. Schullery and 11. Shovic (1989) Burned area survey of Yellowstone National Park: the fires of 1988, Yellowstone National Park, Wyoming, U ,S. Depa rtment of the Interior, National Park Service, Yellowstone National Park, 14p.

Despain, D. (1989) The Yellowstone Fires. Scientific American, 261:376.

Despain, D. G., 1). 1,. Clark, J, J. Reardon (1 996) Simulation of crown fire effects on canopy seed bank in lodgepole pine. International Journal of Wildland Fire. In press.

Freeman A., and 8 others (1995) SIR-C data quality and calibration results, [f '.'I','J,' *Trans. Geosc. Rem. Sells.* 33(4), 848-857.

Holecz F., E. Meier, J. Piesbergen, D. Nuesch and J. Moreira (1994) Rigorous derivation of the backscattering coefficient, *IEEE Trans. Geosc. Rem. Sens. Newsletter* 92, 6-14.

Rignot, E. and R, Chellappa, (1992) Segmentation of polarimetric synthetic aperture radar data, *IEEE Trans. Imag. Proc.* 1, 281 -300."

Romme, W.]]. and D. G. Despain (1989) Historical perspective on the Yellowstone fires of 1 988; BioScience 39:695-699.

Romme, W.]]., 1). G. Despain (1 989) The long history of fire in the Greater Yellowstone Ecosystem. Western Wildlands. 15:17.

Rothermel, R. C., R.A. Hartford, and C. II. Chase (1994) Fire growth maps for the 1988 Greater Yellowstone Area Fires, U.S. Department of Agriculture, Intermountain Research Station, Ogden Utah, INT-304., 1994.

Schullery, 1'. (1989) Yellowstone fires: A preliminary report, *Northwest Science*, 63, 44-51.

Vail Zyl, J .J . (]993)] 'he effect Of topography on radar scattering from vegetated areas, *IEEE Trans. Geosc. Rem. Sens.* 31(1), 1 5:)-1 60.

van Zyl, J.J. (1 992) Application of Cloude's target decomposition theorem to polarimetric imaging radar data, *Proc. SPIE* Vol, 1748 Radar Polarimetry, pp. 184-191.

Table 1. Radar backscatter characteristics of several types of land cover at L-band HH (σ^o_{HH} L), L-band HV (σ^o_{HV} L) and C-band HH (σ^o_{HH} C) expressed in dB.

σ^o_{HH} L	σ^o_{HV} L	σ^o_{HH} C	Type of land cover
-32.8	-39.4	-26.1	Open water
-21.7	-30.3	-18.0	Meadow/Non-forest
-16.5	-25.5	-17.3	Canopy [illegible]
-13.4	-23.0	-14.3	Canopy Burn in Sparse forest
-15.2	-23.5	-15.8	Mixed Burn
-14.9	-23.4	-17.2	Very sparse LP
-12.8	**-21.5**	**-16.5**	Sparse **1,1'**
-14.1	-20.7	-16.1	Intermediate LP
-12.8	-19.9	-16.2	Dense LP

Figures

Figure 1. False color-composite image of the Yellowstone National Park, Wyoming, acquired by SIR-C SAR in October 1994 prior to geocoding.

Figure 2. Geocoded SIR-C imagery after re-calibration and georeferencing of the data to a USGS DEM.

Figure 3. Geocoded SIR-C imagery obtained after reduction of the influence of' the radar illumination angle on radar backscatter assuming a cosine-scattering law.

Figure 4. Map of land cover obtained from SIR-C showing open water, meadows/non-forests, sparse/damaged live lodgepole pine forest, very sparse lodgepole pine of low crown biomass, sparse lodgepole pine of intermediate crown biomass, dense lodgepole pine forest of high crown biomass, canopy burn of no crown biomass, and mixed burn of very low crown biomass. White areas contain no data or correspond to shadowed regions.

Figure 5. Cloude decomposition of the polarimetric signal at P-band (top left corner), L-band (top right corner), and C- band (bottom left corner) frequencies for a 10 km by 10 km SAR scene acquired by the NASA/JPL AIR SAR airborne instrument near old Faithful in September 1989. Red is double bouncing, green is volume scattering, and blue is single bouncing.

Figure 6. Map of fire severity and vegetation inferred from Landsat imagery, aerial photos, and field observations over the area imaged by SIR-C SAR in October 1994.

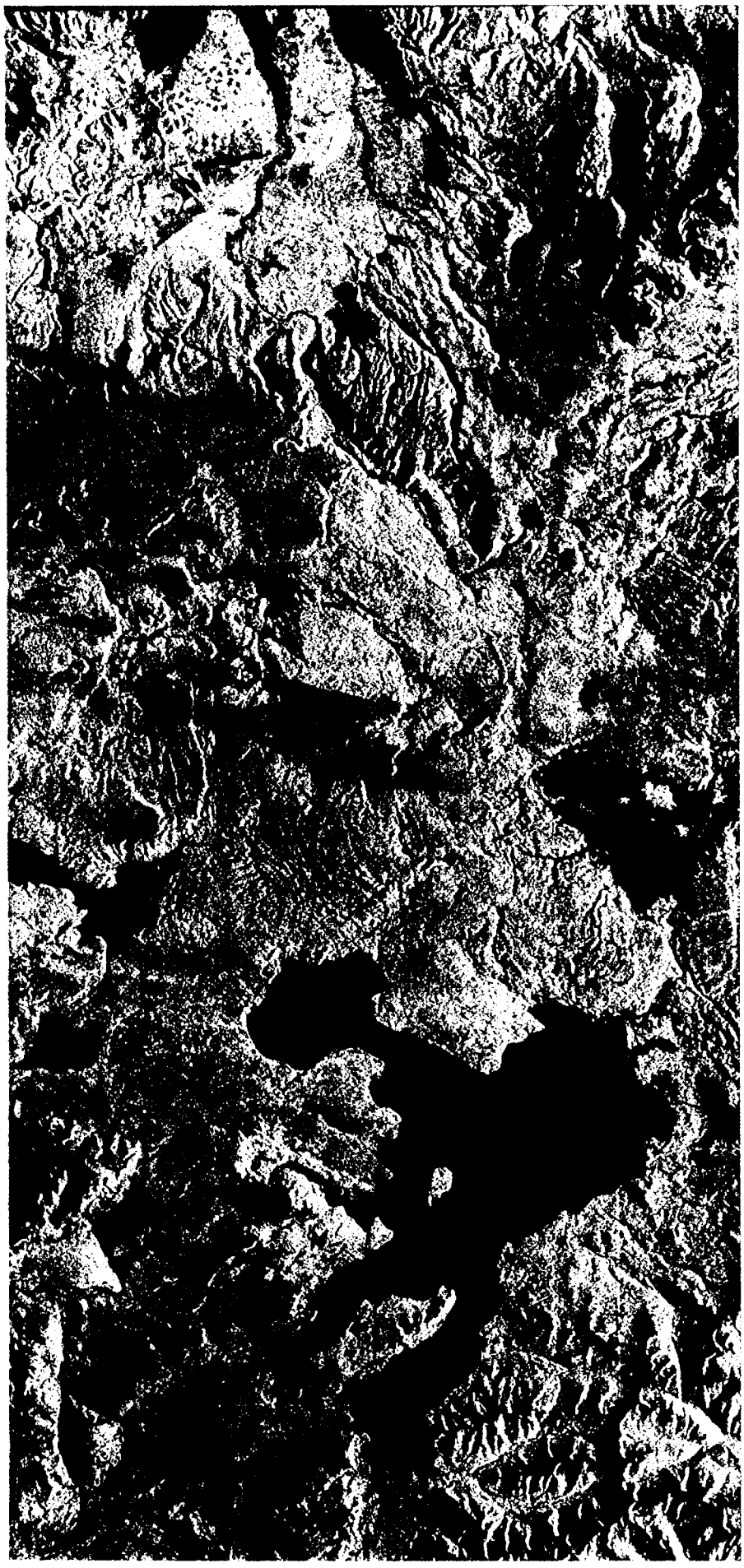

Figure 1.

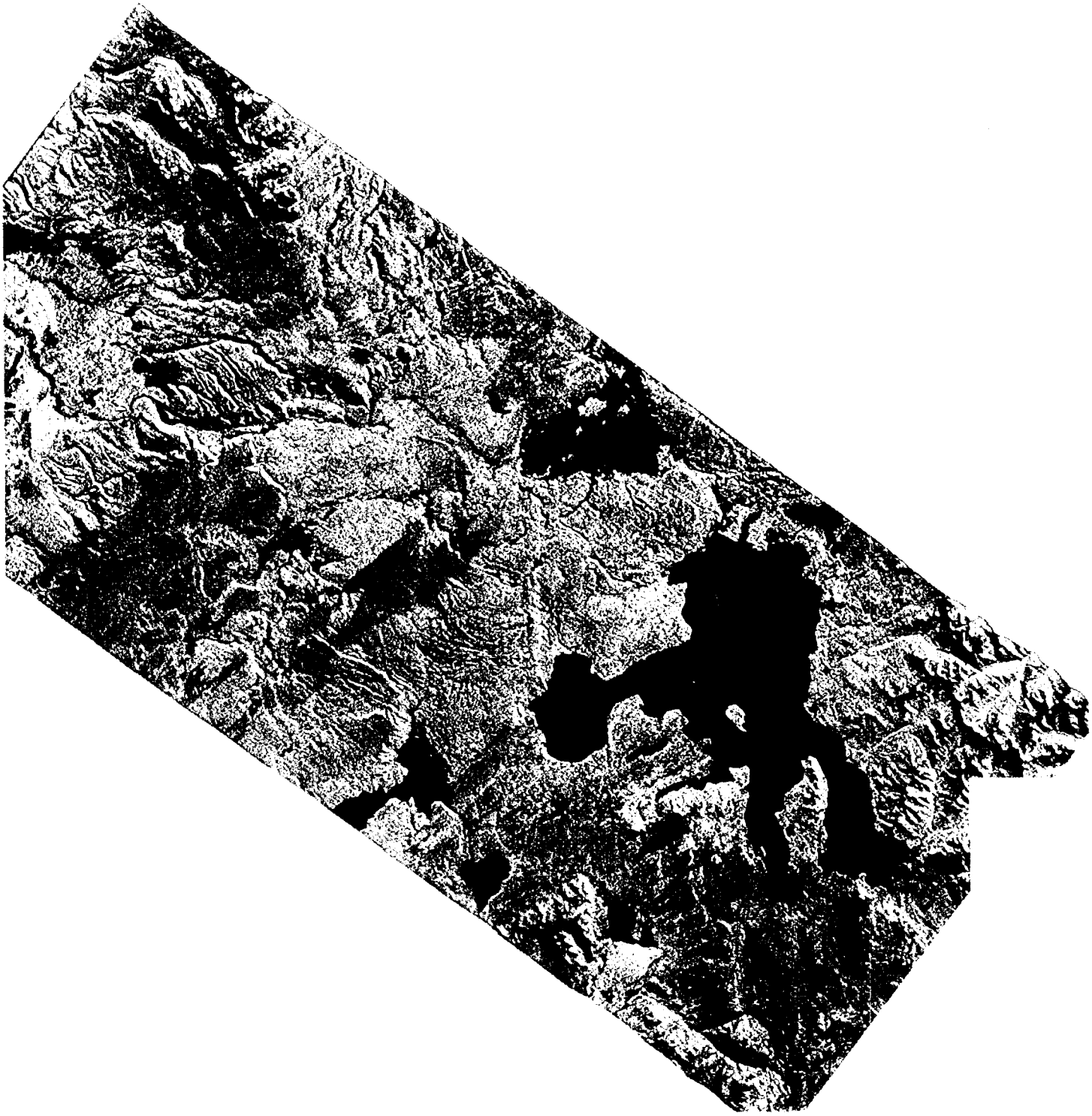

Figure 2. Rignot, Despain and Holecz, 1996

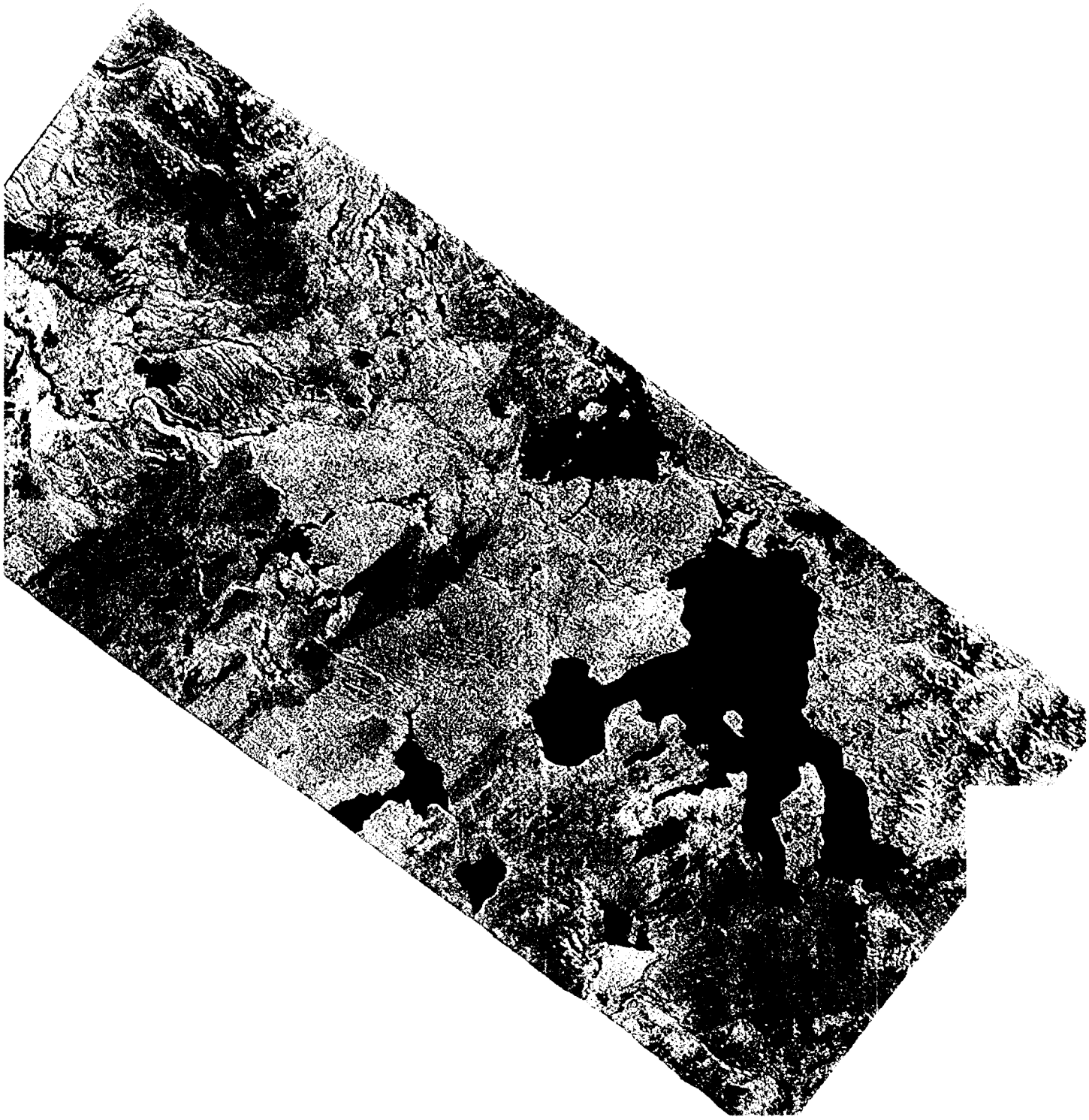

Figure 3. Rignot, Despain and Holecz, 1996

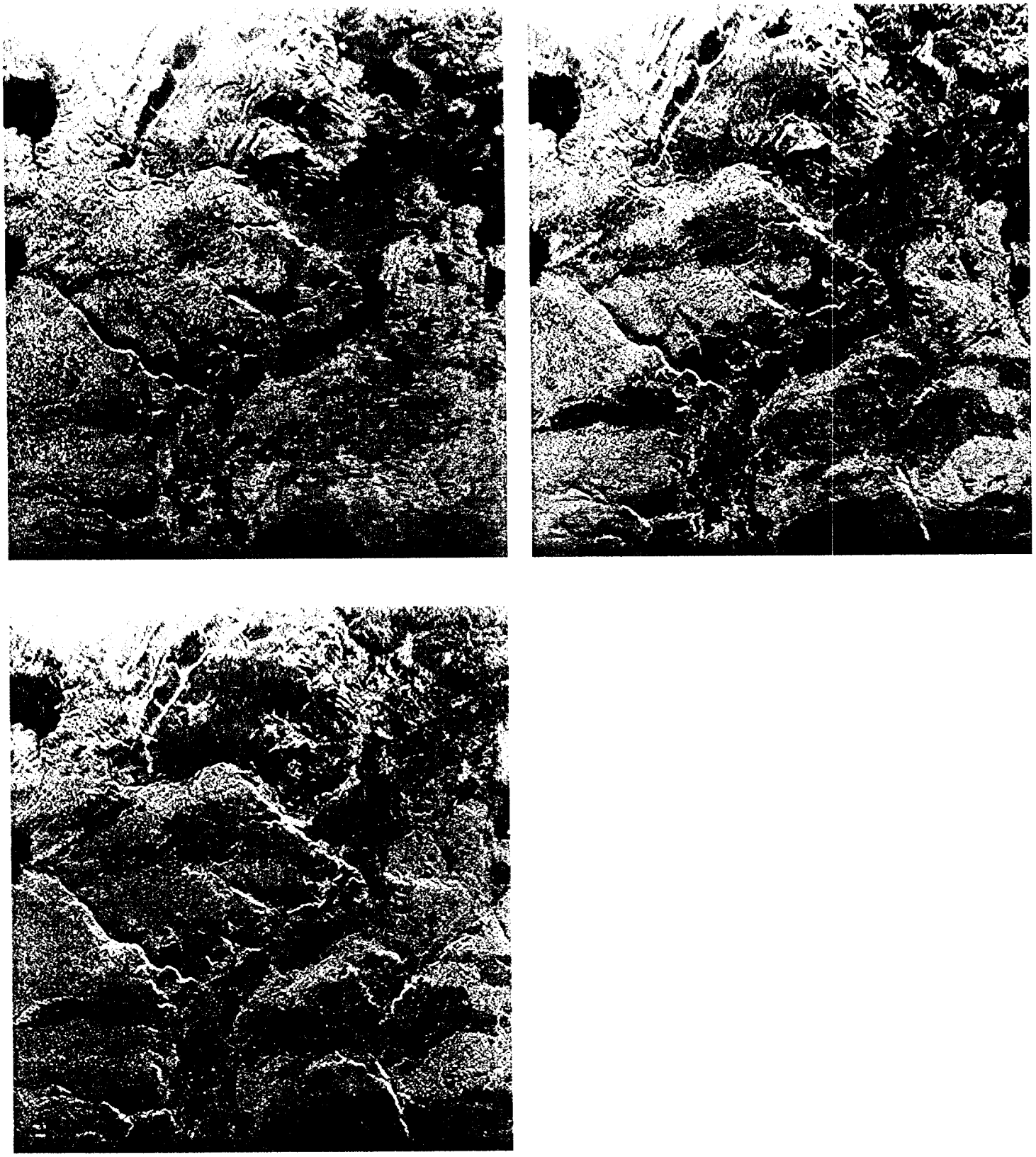

Figure 4. Rignot, Despain and Holecz, 1996

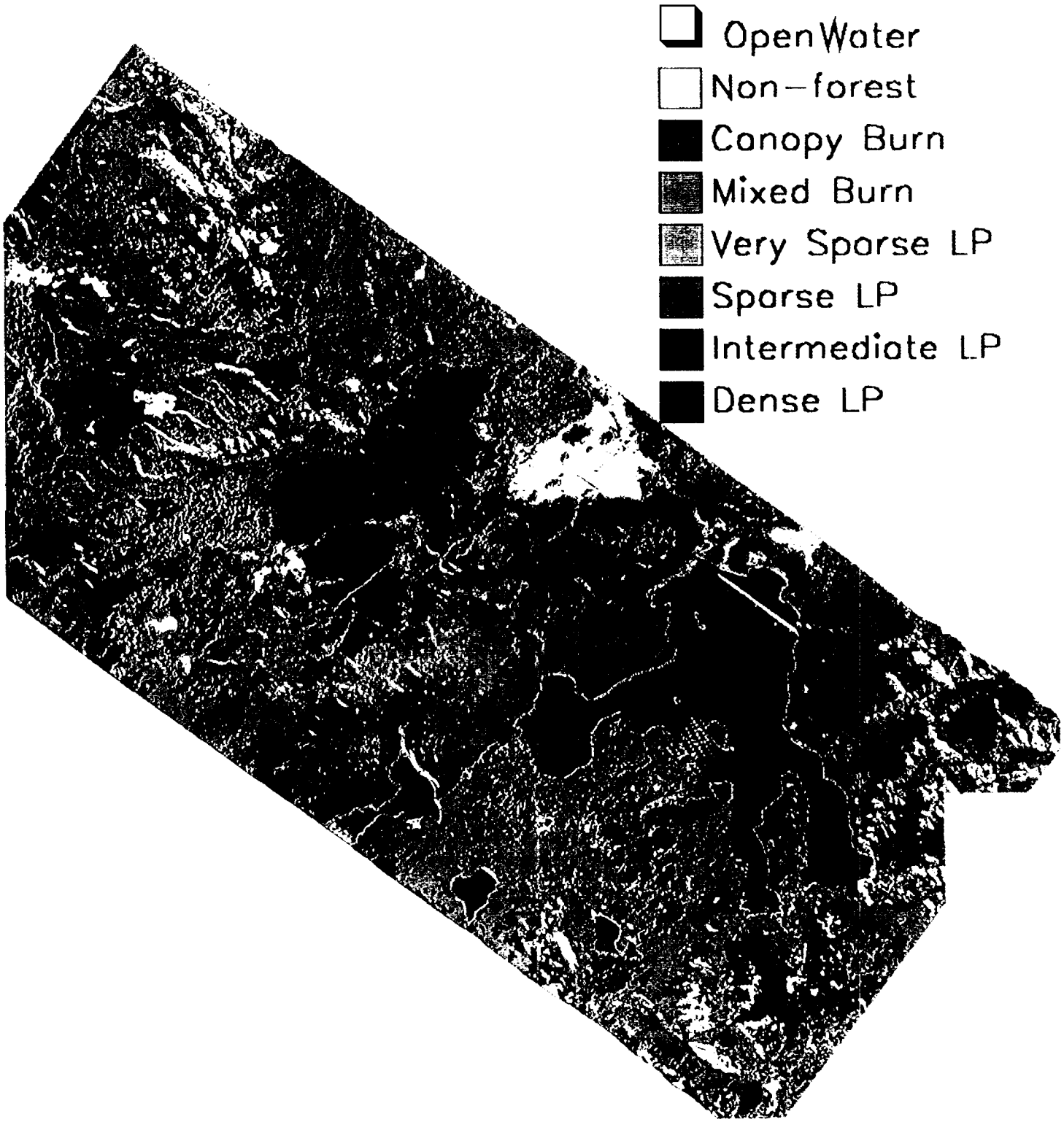

Figure 5. Rignot, Despain and Holecz, 1996

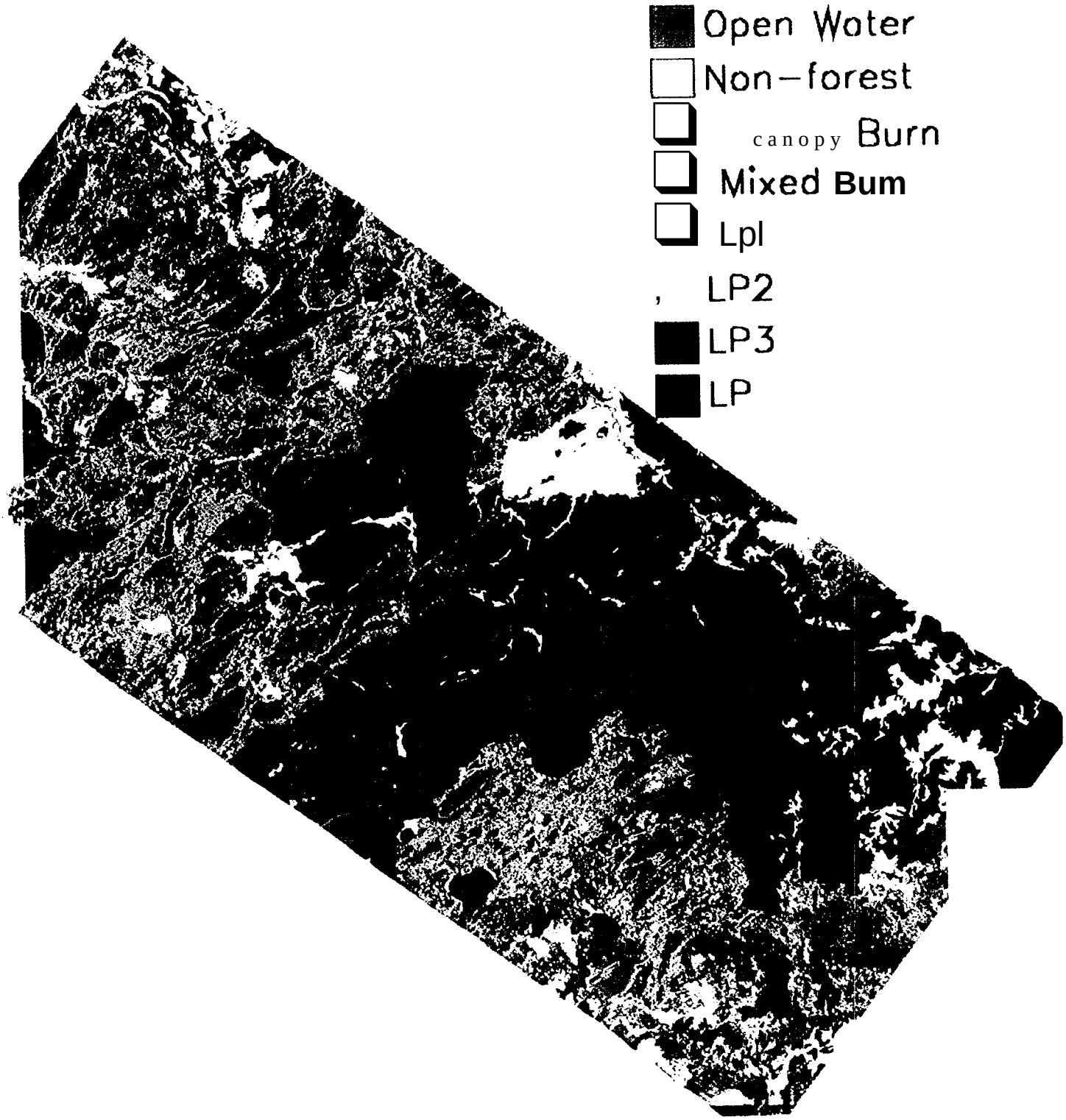

Figure 6. Rignot, Despain and Holecz, 1996